Published in final edited form as:
J Neurovirol. 2013 February ; 19(1): 10–23. doi:10.1007/s13365-012-0135-9.

Patterns of White Matter Injury in HIV Infection after Partial Immune Reconstitution: A DTI Tract-Based Spatial Statistics Study

Tong Zhu[1], **Jianhui Zhong**[1], **Rui Hu**[2], **Madalina Tivarus**[1], **Sven Ekholm**[1], **Jaroslaw Harezlak**[4], **Hernando Ombao**[5], **Bradford Navia**[6], **Ron Cohen**[7], and **Giovanni Schifitto**[1,3]

[1]Dept. Imaging Sciences, University of Rochester, Rochester, New York, USA

[2]Dept. Biostatistics and Computational Biology, University of Rochester, Rochester, New York, USA

[3]Dept. Neurology, University of Rochester, Rochester, New York, USA

[4]Division of Biostatistics, Indiana University School of Medicine, Indianapolis, Indiana, U.S.A.

[5]Dept. Statistics, University of California at Irvine, Irvine, California, U.S.A

[6]Tufts University School of Medicine, Boston, Massachusetts, USA

[7]Brown University, Providence, Rhode Island, U.S.A

Abstract

HIV infected individuals with severe immune suppression are more likely to develop HIV-associated neurocognitive disorders than those with preserved immune function. While partial immune reconstitution occurs in those with severe immune suppression after starting combined antiretroviral therapy, it is not established whether improvement in immune function reverses or prevents injury to the central nervous system (CNS). To address this question, 50 participants (nadir CD4 counts ≤200cells/mm^3, on a stable antiretroviral regimen for at least 12 consecutive weeks prior to study) and 13 HIV negative participants underwent a comprehensive neurological evaluation followed by diffusion tensor imaging (DTI). 84% of the 50 HIV participants were neurologically asymptomatic (HIVNA) and 16% had mild cognitive impairment (HIVCI). Tract-Based Spatial Statistics (TBSS) on DTI data revealed that mean diffusivity (MD) increased significantly in the posterior aspect of both hemispheres in HIVNA compared to controls. In HIVCI, compared to controls and HIVNA, increased MD extended to prefrontal areas. Fractional anisotropy (FA) decreased only in HIVCI, compared to either controls or HIVNA. Furthermore, DTI showed significant correlations to duration of HIV infection and significant associations with multiple cognitive domains. This study highlights that in partial immune reconstitution, injury to the CNS is present even in those that are neurologically asymptomatic and there are discrete spatial patterns of white matter injury in HIVNA subjects compared to HIVCI subjects. Our results also show that quantitative analysis of DTI using TBSS is a sensitive approach to evaluate HIV-associated white matter disease and thus valuable in monitoring central nervous system injury.

Corresponding author: Giovanni Schifitto Department of Neurology and Imaging Sciences University of Rochester 1325 Mount Hope Avenue, Suite 160 Rochester, NY, 14620, U.S.A. Tel: 585-275-3052 Fax: 585-276-1870 Giovanni_Schifitto@URMC.Rochester.edu.

Keywords

Diffusion tensor imaging; HIV infection; white matter njury; cognitive impairment

INTRODUCTION

The introduction of combination antiretroviral therapy (cART) in the mid 1990s has dramatically increased the life expectancy of HIV-infected individuals. The DHHS Panel on Antiretroviral Guidelines for Adults and Adolescents recommends starting antiretroviral therapy for HIV infection if the lymphocyte CD4+ T cell count is ≤ 500mm^3 (http://www.aidsinfo.nih.gov/ContentFiles/AdultandAdolescentGL.pdf.). The recommendation is based on studies suggesting better outcomes in morbidity and mortality associated with HIV infection. However, the increased survival may be unmasking an increase in HIV-associated neurocognitive disorders (HAND) (Antinori et al. 2007) which affect nearly 50% of HIV infected individuals although about 70% of individuals with HAND do not appear to have a measurable functional deficit (Heaton et al. 2010). The persistence of cognitive impairment may be in part due to acquired cognitive deficits at the time of significant immune suppression that is not reversible with the improvement of immune function.

Early studies in advanced HIV disease have shown pathological changes in both gray and white matter (Navia et al. 1986; Budka et al. 1991; Masliah et al. 2000) and that the most likely driver of the central nervous system (CNS) injury is the inflammatory host response to HIV infection (Budka et al. 1987; Tyor et al. 1992). In this regard, increased levels of pro-inflammatory cytokines are more likely to be found in the brain of patients with pre-mortem diagnosis of HIV-associated dementia (Wesselingh et al. 1993). While the degree of CNS inflammation is greatly reduced in patients with good virological control (Clifford et al. 2002; McArthur et al. 2004), it is not known to what extent immune reconstitution in subjects with previously documented severe immune suppression, is associated with “normalization” of CNS injury. Recent studies have shown the persistence of altered brain metabolites and decreased gray and white matter volume in patients with partial immune reconstitution (Cohen et al. 2010a; Cohen et al. 2010b; Harezlak et al. 2011; Tate et al. 2011).

White matter (WM) injury is an integral part of HIV-associated neuropathology (Navia et al. 1986; Budka et al. 1991; Masliah et al. 2000) that can lead to diminishing myelin sheath thickness (Wohlschlaeger et al. 2009) and to frank myelin loss (Bell 1998). Diffusion tensor imaging (DTI) is especially sensitive to differences in WM microstructure. Quantitative information derived from the tensor, for example the extent of diffusion as described by mean diffusivity (MD) and directional dependency of diffusion expressed by fractional anisotropy (FA), can be used to infer non-invasively underlying WM microstructures and anatomical architectures as well as alternations of WM integrity due to pathological conditions.

Previous DTI studies based on region-of-interest (ROI) analyses have reported significant changes in the corpus callosum (Filippi et al. 2001; Thurnher et al. 2005; Wu et al. 2006; Chang et al. 2008), frontal WM (Pomara et al. 2001; Cloak et al. 2004; Wu et al. 2006; Chang et al. 2008), internal capsule (Pomara et al. 2001) and basal ganglia (Ragin et al. 2005; Chang et al. 2008). Other approaches that also include DTI fiber tracking and are often referred to as tract-of-interest (TOI), have similarly shown changes in callosal association and projection of fiber bundles (Pfefferbaum et al. 2009; Tate et al. 2010).

Effective use of ROI and TOI to detect significant changes in the brain relies on the correct selection of these regions. Furthermore, it limits the longitudinal analyses to the same regions while the disease process may be spreading to other areas. Traditional whole brain voxel-based methods have no regional limitation and better efficiency and reproducibility. However, these methods suffer from lower sensitivity than the ROI approach due to the need for inter-subject registration, the randomness in selection of image smoothing level, increased Type I errors (false positives) due to imperfect registration, and reduced statistical power from multiple-comparison corrections (Smith et al. 2006). Tract-Based Spatial Statistics (TBSS, Smith et al. 2006) aims at addressing the limitations of both ROI-based and voxel-based approaches. By generating a whole-brain WM skeleton that represents the center of WM fiber bundles common to all subjects investigated, TBSS not only achieves a more accurate inter-subject spatial alignment but also retains the objectivity of a typical voxelwise analysis and subsequently its explorative power within the whole brain white matter. Therefore, it is potentially more sensitive to diffuse brain WM abnormality as it occurs in HIV-associated CNS injury.

So far, most DTI studies of HAND have focused on showing whether there are differences in brain white matter between HIV-infected individuals and normal controls. However, no careful evaluation has been conducted on the impact of partial immune reconstitution on CNS microstructure. Specifically, is there permanent CNS injury in individuals with previously documented severe immune suppression (typically nadir lymphocytic CD4 cell counts ≤ 100cells/mm^3), when their CD4 count improves significantly under cART treatment? Are some brain areas more vulnerable than others based on objective evidence from imaging? What is the relationship between the spatial distribution of WM injury and cognitive performance?

In light of the above issues, we investigated the effect of partial immune reconstitution on microstructural damages of white matter, as measured by diffusion tensor-derived parameters, in HIV infected subjects with and without cognitive impairment. Using three groups that included healthy controls and HIV infected participants with and without mild cognitive impairment, we examined three hypotheses with TBSS analysis of diffusion tensor-derived parameters.

First, we hypothesized that there would be diffuse WM injuries (measured by decreased FA and increased MD) in HIV-infected individuals even on a stable antiretroviral regimen and without cognitive impairment. Using group comparisons of tensor-derived parameters with TBSS analysis, we expected both extended spatial distribution and increased severity of WM injuries in cognitively impaired individuals.

Further, we hypothesized that DTI parameters could provide objective measures and anatomical information that could distinguish the cognitive asymptomatic stage from the cognitive impaired stage.

Finally, we hypothesized that changes of WM integrity revealed by DTI data would have clinical and cognitive relevance. Here, we hypothesized that the relationship with clinical variables such as duration of HIV infection would not be restricted to specific WM regions reflecting diffuse WM injury in the CNS. By contrast, we expected more specificity between changes in white matter structures, as measured by DTI, and different cognitive domains.

MATERIALS AND METHODS

Participants

Fifty HIV infected individuals (HIV+) and 13 age-matched normal controls were enrolled at the University of Rochester (Rochester, NY, USA), a participating site of the HIV Neuroimaging Consortium (Harezlak et al. 2011). The study was approved by the local institutional review board and participants were enrolled after informed consent was obtained. Inclusion criteria consisted of: nadir CD4 counts ≤ 100cells/mm^3 (later modified to ≤ 200cells/mm^3), stable antiretroviral regimen for at least 12 consecutive weeks prior to study screening, hemoglobin ≥ 9.0 gm/dL, serum creatine ≤ 3 × ULN, AST (SGOT), ALT (SGPT), and alkaline phosphatase ≤ 3 × ULN, negative serum or urine pregnancy test and age ≥ 18 years.

Patients were excluded if they were actively abusing drug and alcohol within 6 months of study entry and had history of severe premorbid or comorbid psychiatric disorders, confounding previous or concurrent neurologic disorder unrelated to HIV infection, such as stroke, head trauma resulting in loss of consciousness > 30 minutes, multiple sclerosis, history of brain infection (except for HIV-1) and brain neoplasm. Control subjects were evaluated in a similar manner and excluded if they had cognitive impairment or any of the confounding risk factors listed above for the HIV infected group.

Patients underwent a comprehensive neurological and neuropsychological evaluation recommended by the updated research nosology for HIV-associated neurocognitive disorders (Antinori et al. 2007). The neuropsychological tests investigated seven cognitive domains, Speed of Information Processing, Verbal Fluency, Working Memory, Verbal Memory, Learning, Executive Function and Motor Speed. The raw test scores of each cognitive domain were converted to deficit scores using established normative data. Summary Z-scores were then calculated for the correlation analysis between cognitive test scores and DTI-derived parameters. In addition, the neurological and neuropsychological evaluation was used to classify HIV infected individuals according to the AIDS Dementia Complex (ADC) staging. An ADC of 0 or 0.5 identifies patients that are neurologically and functionally asymptomatic (HIVNA, n=42) while an ADC ≥1.0 reflects the presence of both cognitive and functional impairment (HIVCI, n=8). These patients would usually fall within the HIV-associated mild neurocognitive disorder using the HIV-associated neurocognitive disorders classification (Antinori et al. 2007).

Laboratory assessments included standard hematology and chemistry profile as well as CD4 count and plasma viral load. Duration of HIV infection was considered as the time from initial HIV infection diagnosis.

DTI Scan Protocol

DTI scans were performed on a GE 1.5T scanner (General Electric, Milwaukee, WI, USA, HDX with 14M software) using a single-shot EPI sequence with twice-refocused spin echoes. The scanning parameters for DTI acquisitions were: TR/TE=7000/75ms, slice thickness=5 mm with no gap, data matrix=128×128, FOV=256×256mm, Array Spatial Sensitivity Encoding Technique (ASSET) factor=2, diffusion weighted images were acquired along 21 non-collinear and non-coplanar directions with b=1000 s/mm^2, and one b=0 s/mm^2 image.

DTI Image Pre-processing

A custom software tool based on Matlab (The Mathworks, Natick, MA, USA), R language (R Foundation for Statistical Computing, http://www.R-project.org), C++ and various

functions in the FSL package (FMRIB Analysis Group, Oxford University, Oxford, UK; Smith et al. 2004) was used for image processing and statistical analysis.

For each participant, three processing steps were performed on DTI. First, artifacts due to eddy current and subject's movement were simultaneously removed using the EddyCorrect tool of FSL. Second, tensor-derived parametric maps, FA, MD, axial diffusivity (AD) and radial diffusivity (RD), were estimated using the DTIFIT tool. Lastly, FA maps were fed into the TBSS tool to generate the white matter skeleton. Corresponding skeletonized maps for MD, AD and RD were similarly generated. Voxelwise statistical analyses of DTI data, including voxelwise cross-subject comparisons and correlation analyses, were further performed within the skeleton.

Spatial Classifications of DTI Changes Using DTI Atlases

Two DTI atlases included in the FSL package, the John Hopkins University ICBM-DTI-81 White Matter Atlas (referred as the WM Atlas henceforth) and the White Matter Tractography Atlas (referred as the Tract Atlas henceforth), were chosen as templates for identification of major WM structures/fiber pathways. The WM Atlas (Mori et al. 2005) includes 50 major WM structures with bilateral parts of the same structure labeled separately. There are 20 major WM fiber tracts in the Tract Atlas. In this study, the nomenclature and names for each WM structure/pathways in the atlases follow those used by Mori et al., 2005. The information of WM structures/pathways from the two atlases is complementary thus providing comprehensive identification of major WM regions and fiber pathways.

Voxelwise Group Comparisons of DTI Parameters Using TBSS Analysis

For each tensor-derived parameters (FA, MD, AD, RD), three group comparisons were performed, HIVNA vs. controls, HIVCI vs. controls, and HIVCI vs. HIVNA. Group differences in the tensor-derived parameters were detected by permutation tests using the Randomize toolbox in FSL. Correction for multiple comparisons was performed using the threshold-free cluster enhancement (TFCE) approach in FSL (Smith et al. 2009) to achieve significance level at $p<0.05$.

Anatomical regions in the skeleton showing significant group differences in the tensor-derived parameters were then identified and labeled according to structures defined in the WM Atlas. To quantify the scale of WM abnormality (in terms of both spatial extension and severity) associated with HIV infection, a quantitative measure, the percentage of skeleton abnormality (*Skeleton_Abnorm%*), was calculated for each structure defined in the WM Atlas, using a two-step approach. First, each voxel in skeleton was labeled and assigned to the corresponding structure within the WM atlas to form a skeletonized atlas. The total number of voxels that belong to the same structure was calculated as Vox_Sum_i (i represents 50 WM structures defined in the WM Atlas, i=1,2,…,50). Second, for each structure within the skeleton, the total number of voxels in which significant voxelwise group differences of DTI parameters were detected by TBSS analyses was calculated as $Abnorm\_Vox\_Sum_i$. The percentage of skeleton abnormality value for a WM structure within the WM atlas was then calculated as

$$(\text{Skeleton\_ Abnorm\%})_i = \frac{(\text{Abnorm\_ Vox\_ Sum})_i}{(\text{Vox\_ Sum})_i} \times 100\%, \text{ where } i=1, 2, \ldots, 50.$$

Classification of HIVCI, HIVNA and Normal Individuals using DTI Parameters

In order to assess this aim, binary logistic regression analyses were applied to WM structures with significant group differences in DTI measures to further select WM structures with highest sensitivity, specificity and accuracy that differentiated the groups. Diagnostic group based on the ADC score (HIVCI, HIVNA and Control) was considered as the dependent variable and mean tensor-derived parameters were selected as the independent predictor variables. Classification power of tensor-derived parameters from each WM region was assessed by the value of the Area Under Receiver-Operating-Characteristics Curve (AUC). A threshold value of 0.85 for AUC was selected as the criterion for achieving a good discrimination power.

Voxelwise Correlation between DTI Parameters and Clinical Variables for HIV+ Patients

We expected that WM injury would be diffuse in HIV infected individuals and the relationship with clinical variables, such as duration of HIV infection, would also not be restricted to specific WM regions. In order to assess clinical relevance of DTI data, voxelwise correlation analyses were performed between tensor-derived parameters and five clinical variables, nadir CD4+ T cell count, current CD4+ T cell count, plasma HIV RNA concentration and duration of HIV infection, CNS Penetration-Effectiveness (CPE) score (Letendre et al, 2008), for all HIV infected participants using the Randomise toolbox in FSL. Multiple comparisons correction was performed using the TFCE approach to achieve a significance level at $p<0.05$.

ROI-based Association Analysis between DTI Parameters and Cognitive Performance for HIV+ Patients

There are specific structural/functional connections between white matter and gray matter structures that subserve different cognitive domains. To assess cognitive relevance of DTI data, correlation analyses between deficits in neurocognitive performance and FA/MD of HIV+ patients (both HIVCI and HIVNA) were performed for each WM structure where significant changes in FA/MD were observed in the comparisons of HIVNA and HIVCI groups in the TBSS analysis. A Spearman rank correlation analysis was first conducted between each deficit score of the seven cognitive domains and the mean values of FA/MD within the structure. Furthermore, multilinear regression analyses with model selection were conducted to detect the multilinear association between deficit scores (as independent predictors) and mean values of FA/MD (as dependent outcomes). The model selection was conducted by using the stepwise forward procedure. The p value for the entrance and exit tolerance of a performance score in model selection was set to be 0.05 and 0.1 separately.

RESULTS

Eighty-four percent (42/50) of the randomly enrolled HIV infected subjects with a nadir CD4 count ≤ 200 cells/mm^3 (35/42 with nadir CD4 count ≤ 100 cells/mm^3) were neurologically asymptomatic and 16% (7/8 with nadir CD4 count ≤ 100 cells/mm^3) had cognitive impairment (Table 1). Forty-five of the 50 subjects had documented cART history with 34 HIVNA and 7 HIVCI on cART at the time of the evaluation. There is no significant group difference in terms of the percentage of subjects underwent cART (p=0.68 from Wilcoxon Rank Sum test). A current CD4 count over 200 was achieved by 88% of HIVNA and by 50% of HIVCI. Overall, patients with cognitive impairment were more likely to have both a lower nadir and current CD4 count. HIV RNA was detectable in 9/42 (22.4%) of HIVNA and 3/8 (37.5%) of HIVCI patients; however, only 4 HIVNA patients, and one HIVCI patients, had plasma HIV RNA above 10,000 copies/ml. No significant differences in age ($P_{HIVNA\ vs.\ Control}=0.99$, $P_{HIVCI\ vs.\ Control}=0.25$, $P_{HIVCI\ vs.\ HIVNA}=0.32$) were detected among groups. There was a significant gender difference among groups with all three p

values smaller than 0.01 (Wilcoxon Rank Sum test). Given the relatively small sample size in this study, both age and gender effects were adjusted by including them as covariates in TBSS analyses.

White Matter Abnormalities in HIV+ Patients

TBSS analysis shows significant differences in DTI parameters of HIV infected individuals compared to HIV negative controls. These differences are more evident in the HIVCI group as shown in Table 2 and Fig.1.

When comparing the HIVNA group (ADC 0 and 0.5) with controls, significantly increased MD values are observed only within WM structures that are either primarily localized in the posterior area of the frontal lobe, the temporal lobe and the parietal lobe or contain fiber pathways mainly associated or connected to the posterior areas of the frontal lobe and the parietal lobe (Table 2, top half). These regions include the body and splenium of corpus callosum (containing the posterior frontal and parietal section of callosal fibers, such as the forceps major), the bilateral superior and posterior corona radiata (containing sections of both cortico-efferent and cortico-afferent projection fibers superior to the internal capsule), the posterior thalamic radiation (containing the parietal and occipital section of the cortico-afferent projection fibers, such as the optical tracts and the parietal thalamocotical fibers), the bilateral sagittal stratum (containing association fibers, such as the inferior longitudinal fasciculus and the inferior fronto-occipital fasciculus) and the bilateral superior longitudinal fasciculus. In contrast, there were no significant FA differences between the HIVNA and the control group.

With clinically manifested CNS injury (ADC≥ 1), both spatial extension (measured as the total number of WM structures with significant DTI changes) and severity (measured as the percentage of skeleton abnormality within each WM structure) of WM abnormality are increased. More skeleton voxels with significant abnormality in MD are seen within these abovementioned WM structures (indicated by increased values of *Skeleton_Abnorm%* in Table 2). Abnormality in MD within the posterior frontal, temporal and parietal lobes have also spread to more WM structures, including bilateral parts of the posterior limb of internal capsule, the external capsule and the superior fronto-occipital fasciculus. More interestingly, significantly increased MD values were observed exclusively in HIVCI subjects in several WM structures within the prefrontal lobes (Fig. 1 and the bottom half of Table 2,), including the genu of the corpus callosum (containing the forceps minor), bilateral parts of the anterior limb of internal capsule, the cingulum and the anterior corona radiata (containing thalamocortical fibers that connect the anterior and medial nuclei of the thalamus to the prefrontal cortex).

While MD changes were present throughout the spectrum of the disease, FA changes became significant only in cognitively impaired patients in WM structures that contain fiber pathways mainly associated or connected to the prefrontal cortex. These structures include the genu of the corpus callosum, the bilateral anterior corona radiata and the bilateral section of the cingulum around the cingulate gyrus.

Increases in AD and RD values are also present throughout the course of the HIV infection (Fig. 2). An elevated RD value was observed in most skeleton locations that exhibited significantly increased MD values within either HIVNA or HIVCI groups. In contrast, increase in AD was less prevalent, in terms of both spatial extension and severity (Fig. 2 and Table 2).

Classification of HIVCI, HIVNA and Normal Individuals Based on TBSS

Both MD and RD values of four WM structures within the temporal and parietal lobes are sensitive discriminators between normal and HIVNA participants (Table 3). These regions include the splenium of corpus callosum, the bilateral posterior thalamic radiation and the left superior longitudinal fasciculus. Among these structures, the overall classification accuracy using MD is 85.5%±9.75% (with a sensitivity value of 82.5%±8.58% and a specificity value of 84.8%±6.13%) and the overall classification accuracy using RD is 80.8%±4.27% (with a sensitivity value of 79.0%±7.39% and a specificity value of 86.5% ±7.14%).

MD in the body of corpus callosum, the bilateral section of the cingulum in the cingulate gyrus, the bilateral anterior and posterior limb of the internal capsule and the bilateral external capsules show consistent discriminating power in the classification of HIVNA and HIVCI patients (Table 4). The average classification accuracy using MD information is 84.9%±6.09% (with a sensitivity value of 89.1%±13.0% and a specificity value of 84.1% ±8.68%). In addition, the FA value in the body of the corpus callosum discriminates HIVNA from HIVCI individuals with a classification accuracy of 82.0%, a sensitivity value of 88.0% and a specificity value of 81.0%.

Voxelwise Correlation between DTI Parameters and Clinical Variables for HIV+ Patients

Among five common clinical variables, only duration of HIV infection had significant correlations with DTI parameters as shown in Fig. 3 and Table 5.

Regions where both FA and MD show significant correlations include the corpus callosum (including callosal fiber pathways and the section of the cingulum pathways near the cingulate gyrus), bilateral anterior coronal radiata (involving the forceps minor, the prefrontal section of the superior longitudinal fasciculus and the prefrontal section of the anterior thalamic radiation that connects the anterior and medial nuclei of the thalamus to the prefrontal cortex), bilateral superior corona radiata (involving the corticofugal pathways, such as the corticospinal tracts, and the posterior frontal section of the anterior thalamic radiation) and bilateral posterior corona radiata (involving the inferior fronto-occipital fasciculus and the inferior longitudinal fasciculus pathways within the temporal lobe). Additional clusters with significant correlations only between MD and disease duration include bilateral posterior thalamic radiation (involving the section of the inferior fronto-occipital fasciculus and the inferior longitudinal fasciculus pathways within the occipital lobe) and the left external capsule (involving both the uncinate fasciculus and the inferior fronto-occipital fasciculus within the inferior and dorsal frontal lobe).

ROI-based Association Analysis between DTI Parameters and Cognitive Performance of HIV+ Patients

The Spearman correlation analysis indicated that two cognitive domains, Speed of Information Processing and Verbal Fluency, were significantly correlated with FA/MD. These results were further confirmed in a multilinear regression analysis with model selection (Table 6). Reduced scores in these domains (i.e. increased deficit scores) were significantly associated with either reduced FA or elevated MD across multiple WM structures, including the body and splenium of the corpus callosum, the anterior limb of the internal capsule (left), the anterior (left), superior (left) and posterior corona radiata (bilateral), the posterior thalamic radiation (left), the external capsule (bilateral), the superior longitudinal fasciculus (left), and the superior fronto-occipital fasciculus (bilateral).

It is worth noting that these associations tended to be lateralizing to the left hemisphere for Verbal Fluency and included areas such as the left superior longitudinal fasciculus and the

left inferior fronto-occipital fasciculus. By contrast, WM structures with significant associations between DTI and Speed of Information Processing tended to be more diffuse, involving both hemispheres.

For most regions in which significant correlation between MD and clinical/cognitive scores were observed, there were also significant positive correlations with RD. No significant correlation between AD and any clinical/cognitive variables was detected.

DISCUSSION

The results of this study highlight that, in the context of immune reconstitution, there is evidence of diffuse white matter abnormalities in HIV infected individuals, even in those who are neurologically asymptomatic. Given that this was a cross-sectional evaluation, it is possible that white matter lesions occurred at the time of the most severe immune suppression when the host inflammatory response and HIV viral toxicity were at their peak. Therefore, it is possible that what we have observed is a legacy effect, a sign of static WM damage. On the other hand, the correlation that we found with the duration of HIV infection suggests that the process is dynamic and potentially progressive. In this regard, a recent longitudinal morphometric study also suggests progression of CNS injury (Tate DF et al. 2011).

This study not only confirms but also extends previous DTI finding from ROI and TOI studies in HIV infected individuals. The pattern of WM involvement does not appear random. Specifically, prior to significant cognitive impairment, WM structures involved are either primarily localized in the posterior aspect of the frontal lobes, the temporal lobes and the parietal lobes or contain fiber pathways mainly associated or connected to posterior areas of the frontal and parietal lobes. In fact, using either MD or RD parameters in regions that include the splenium of the corpus callosum, the posterior thalamic radiation and the superior longitudinal fasciculus we can correctly classify HIVNA and controls with an overall accuracy above 80%. The posterior spatial distribution of white matter abnormalities in HIV infected, cognitively asymptomatic individuals revealed in this study is in part consistent with a previous morphometric postmortem study of the corpus callosum in HIV infected non-demented individuals (Wohlschlaeger et al. 2009).

The transition to cognitive impairment is associated with not only an extension of WM abnormalities, now involving even more rostral aspect of the frontal lobes as well as deeper WM structures, but also with a quantitative increase in the burden of WM injuries compared to HIVNA. In this regard, tensor-derived parameters (especially MD and RD), in the body of corpus callosum, the anterior section of cingulum, the internal and external capsules showed an accuracy >80% in distinguishing HIVNA from HIVCI.

Among four DTI parameters investigated in this study, increase in MD, AD and RD were present throughout the spectrum of the disease while FA changes became significant only in cognitively impaired patients. In HIVNA group, increase of AD and RD due to pathological process are relatively small comparing to HIVCI group. In addition, simultaneous increase of AD and RD in the same region (Fig. 2) might cancel out the change in anisotropy measures and further contribute to the low sensitivity and specificity of FA for detecting WM injury associated with neurologically asymptomatic stage.

Overall, it appears that changes in radial diffusivity are more prominent than axial diffusivity. Based on studies in animal models (Song et al. 2002; MacDonald et al. 2007), increased RD is a marker for demyelination. Therefore, our findings would imply that the inflammatory insult to the white matter is predominantly demyelinating while axonal injury co-occurs but to a lesser degree.

However, in the transition to cognitive impairment there is a clearly trend of increase in AD within more WM structures (Fig. 2 and Table 2). This finding is consistent with two previous DTI studies (Chen et al. 2009; Pfeferbaum et al. 2009) and suggests the presence of axonal injury as similar results in chronic WM injury have been reported in neurodegenerative disease where neurons are the primary target including Alzhermer's disease (Agosta et al. 2011), Huntington's disease (Rosas et al. 2010), amyotrophic lateral sclerosis (Metwalli et al. 2010) and Friedreich's ataxia (Della Nave et al. 2010). Therefore, the increase of AD seen in HIV infection and other neurodegenerative disorders is likely the result of a chronic injury, which is in contrast to decreased AD seen in acute injury as shown in studies of rat model with experimentally induced transient retinal ischemia (Sun et al. 2006) or central contusions from controlled cortical impacts (MacDonald et al. 2007). Given that most clinical DTI scans (including this study) use a relatively low b value around 1000 s/mm^2, the diffusion process measured are thought to come primarily from extracellular space rather than within axons (Le Bihan et al. 2001). Any changes of the interstitial space between axons due to pathological processes directly affect AD value. Reduced axon density or caliber will increase the interstitial space and subsequently increases AD values. In this regard, Thompson et al., 2006 found significant ventricular expansion and callosal thinning in HIV infected individuals. Their study also showed that callosal thinning in anterior regions significantly correlated with a decline immune system as measured by CD4+ T cell count. Therefore, the increased AD observed in HIV infection and other neurodegenerative disorders may represent increased extracellular water content secondary to atrophy (Rosas et al. 2010; Agosta et al. 2011).

We also investigated the relationship between DTI parameters and several clinical and laboratory variables including CD4+ T cell count, plasma HIV RNA and duration of HIV infection and CPE scores. We found no significant correlation between DTI parameters and CD4+ T cell count (both nadir and current). These findings may be due to the study design. By inclusion criteria, the spread of nadir CD4 count was relatively small and there was a high percentage of patients achieving a current CD4+ T cell count >200. Patients were on stable cART, most had undetectable or minimally detectable viral load. Similar argument can be made for the lack of correlation with plasma HIV RNA.

We found significant correlations between duration of HIV infection and DTI parameters in several WM structures. This is in part to be expected as the longer the duration of HIV infection, the more opportunity there is for CNS injury. Among these WM structures, involvement of the corpus callosum is of particular interest. As the largest WM connectivity structure in the brain, the corpus callosum is involved in most cognitive processes. Several lines of evidence including morphology (Thompson et al. 2006) and histopathological studies (Gray et al. 1992; Wohlschlaeger et al. 2009) in addition to DTI have all pointed to WM damages in the corpus callosum of HIV infected individuals.

The significant association between performance across several neurocognitive domains and tensor-derived parameters from multiple WM structures suggests that abnormalities of WM integrity have functional consequences. The observation of the functional associations between DTI changes and deficits in Speed of Information Processing in multiple WM structures in this study are consistent with the known literature on the neurocognitive effects of HIV infection (Parsons et al. 2006; Woods et al. 2009). It is also noteworthy that associations between information processing speed and DTI were evident across structurally and functionally divergent white matter systems. This is consistent with the fact that several other domains and therefore pathways may be contributing to deficits in information processing speed, including attention, visual perception, working memory and praxis (Woods et al. 2009). This finding fits with what is known about the importance of cerebral WM for insuring optimal communication across brain areas. WM damage is associated with

slowed cognitive processing across a range of disorders, including multiple sclerosis (Benedict and Zivadinov 2011) and small vessel vascular disease (Jokinen et al. 2011). Our findings support that processing speed deficits may reflect diffuse WM involvement secondary to HIV infection.

In contrast, more selective pathways have been described in verbal fluency deficits. For example, the superior longitudinal fasciculus, the inferior longitudinal fasciculus and the inferior fronto-occipital fasciculus in the left hemisphere, areas where we found associations between Verbal Fluency and DTI parameters, are essential parts of the language network (Duffau, 2008). A recent study combining observations from intra-operative brain stimulations and postsurgical MRI scans has shown that left inferior fronto-occipital fasciculus, the fiber pathway connecting the posterior temporal lobe with the orbitofrontal lobe, plays an essential role in semantic processing, and the inferior longitudinal fasciculus, although not critical for language, also provides an indirect pathway related to verbal processing (Mandonnet et al. 2007). The splenium of the corpus callosum is another area where we found an association between Verbal Fluency and DTI parameters. In this regard, it is of interest that the RD of the temporal-callosal fiber pathway (part of the splenium of the corpus callosum) has been reported to be associated with phonological awareness (Dougherty et al. 2007).

The study has several limitations that need to be considered. The three groups were of unequal sample size with the impaired group being the smallest. While the analyses conducted are of significance even without the inclusion of the impaired group, having this group albeit small, gave us an opportunity to explore the relationship between clinical transition and DTI parameters. Another drawback is that our investigation was restricted to the WM space defined by the atlases in the FSL package, to identify potential CNS injuries with the white matter. Use of more detailed atlases would provide a more comprehensive representation of CNS injury.

The overall results of this study suggest that HIV infected subjects with history of significant immune suppression and partial immune reconstitution have signs of CNS injury despite the lack of clinically manifested signs or symptoms. The unique spatial distribution of WM injury at different stages of HIV infection, as measured by DTI, may provide a useful marker to monitor HIV–associated CNS injury. The association between relevant clinical and functional disease variables and tensor-derived parameters observed in this study provide confirmation that DTI is a valuable biomarker to monitor HAND. A longitudinal follow-up is necessary to establish whether the WM changes observed are permanent, static or progressive.

Acknowledgments

The authors appreciate useful discussions with Dr. Wei Tian of Dept. Imaging Sciences at the University of Rochester.

References

Agosta F, Pievani M, Sala S, Geroldi C, Galluzzi S, Frisoni GB, Filippi M. White Matter Damage in Alzheimer Disease and Its Relationship to Gray Matter Atrophy. Radiology. 2011; 258:853–863. [PubMed: 21177393]

Antinori A, Arendt G, Becker JT, Brew BJ, Byrd DA, Cherner M, Clifford DB, Cinque P, Epstein LG, Goodkin K, Giesslen M, Grant I, Heaton RK, Joseph J, Marder K, Marra CM, McArthur JC, Nunn M, Price RW, Pulliam L, Robertson KR, Sacktor N, Valcour V, Wojna VE. Updated research nosology for HIV-associated neurocognitive disorders. Neurology. 2007; 69:1789–1799. [PubMed: 17914061]

Bell JE. The neuropathology of adult HIV infection. Rev Neurol (Paris). 1998; 154:816–829. [PubMed: 9932303]

Benedict RH, Zivadinov R. Risk factors for and management of cognitive dysfunction in multiple sclerosis. Nat Rev Neurol. 2011; 7:332–342. [PubMed: 21556031]

Budka H, Constanzi G, Cristina S, Lechi A, Parravicini C, Trabattoni R, Vago L. Brain pathology induced by infection with the human immunodeficiency virus (HIV). A histological, immunocytochemical, and electron microscopical study of 100 autopsy cases. Acta Neuropathol. 1987; 75:185–198. [PubMed: 3434225]

Budka H, Wiley CA, Kleihues P, Artigas J, Asbury AK, Cho ES, Cornblath DR, Dal Canto MC, DeGirolami U, Dickson D. HIV-associated disease of the nervous system: Review of nomenclature and proposal for neuropathology-based terminology. Brain Pathol. 1991; 1:143–152. [PubMed: 1669703]

Chang L, Wong V, Nakama H, Watters M, Ramones D, Miller EN, Cloak C, Ernst T. Greater than age-related changes in brain diffusion of HIV patients after 1 year. J. Neuroimmune Pharmacol. 2008; 3:265–274. [PubMed: 18709469]

Chen YS, An HY, Zhu HT, Stone T, Smith JK, Hall C, Bullitt E, Shen D, Lin W. White matter abnormalities revealed by diffusion tensor imaging in non-demented and demented HIV+ patients. Neuroimage. 2009; 47:1154–1162. [PubMed: 19376246]

Clifford DB, McArthur JC, Schifitto G, Kleburtz K, McDermott MP, Letendre S, Cohen BA, Marder K, Ellis RJ, Marra CM, Neurologic AIDS, Research Consortium. A randomized clinical trial of CPI-1189 for HIV-associated cognitive-motor impairment. Neurology. 2002; 59:1568–1573. [PubMed: 12451199]

Cloak CC, Chang L, Ernst T. Increased frontal white matter diffusion is associated with glial metabolites and psychomotor slowing in HIV. J Neuroimmunol. 2004; 157:147–152. [PubMed: 15579292]

Cohen RA, Harezlak J, Schifitto G, Hana G, Clark U, Gongvatana A, Paul R, Taylor M, Thompson P, Alger J, Brown M, Zhong J, Campbell T, Singer E, Daar E, McMahon D, Tso Y, Yiannoutsos CT, Navia B. Effects of nadir CD4 count and duration of human immunodeficiency virus infection on brain volumes in the highly active antiretroviral therapy era. J Neurovirol. 2010a; 16:25–32. [PubMed: 20113183]

Cohen RA, Harezlak J, Gongvatana A, Buchthal S, Schifitto G, Clark U, Paul R, Taylor M, Thompson P, Alger J, Brown M, Zhong J, Campbell T, Singer E, Daar E, McMahon D, Tso Y, Yiannoutsos CT, Navia B, HIV Neuroimaging Consortium. Cerebral metabolite abnormalities in human immunodeficiency virus are associated with cortical and subcortical volumes. J Neurovirol. 2010b; 16:435–444. [PubMed: 20961212]

Della Nave R, Ginestroni A, Diciotti S, Salvatore E, Soricelli A, Mascalchi M. Axial diffusivity is increased in the degenerating superior cerebellar peduncles of Friedreich's ataxia. Neuroradiology. 2011; 53:367–372. [PubMed: 21128070]

Dougherty RF, Ben-Shachar M, Deutsch GK, Hernandez A, Fox GR, Wandell BA. Temporal-callosal pathway diffusivity predicts phonological skills in children. PNAS. 2007; 104:8556–8561. [PubMed: 17483487]

Duffau H. The anatomo-functional connectivity of language revisited new insights provided by electrostimulation and tractography. Neuropsychologia. 2008; 46:927–934. [PubMed: 18093622]

Filippi CG, Ulug AM, Ryan E, Ferrando SJ, van Gorp W. Diffusion Tensor Imaging of Patients with HIV and Normal-appearing White Matter on MR Images of the Brain. AJNR Am J Neuroradiol. 2001; 22:277–283. [PubMed: 11156769]

Jokinen H, Gouw AA, Madureira S, Yikoski R, van Straaten EC, van der Flier WM, Barkhof F, Scheltens P, Fazekas F, Schmidt R, Verdelho A, Ferro JM, Pantoni L, Inzitari D, Erkinjuntti T, LADIS Study Group. Incident lacunes influence cognitive decline: the LADIS study. Neurology. 2011; 76:1872–1878. [PubMed: 21543730]

Gray F, Lescs MC, Keohane C, Paraire F, Marc B, Durigon M, Gherardi R. Early brain changes in HIV infection: neuropathological study of 11 HIV seropositive, non-AIDS cases. J Neuropathol Exp Neurol. 1992; 51:177–185. [PubMed: 1538241]

Harezlak J, Buchthal S, Taylor M, Schifitto G, Zhong J, Darr E, Alger J, Singer E, Campbell T, Yiannoutsos C, Cohen R, Navia B, HIV Neuroimaging Consortium. Persistence of HIV-associated cognitive impairment, inflammation, and neuronal injury in era of highly active antiretroviral treatment. AIDS. 2011; 25:625–633. [PubMed: 21297425]

Heaton RK, Clifford DB, Franklin DR Jr, Woods SP, Ake C, Vaida F, Ellis RJ, Letendre SL, Marcotte TD, Atkinson JH, Rivera-Mindt M, Vigil OR, Taylor MJ, Collier AC, Marra CM, Gelman BB, McArthur JC, Morgello S, Simpson DM, McCutchan JA, Abramson I, Gamst A, Fennema-Notestine C, Jernigan TL, Wong J, Grant I, CHARTER Group. HIV-associated neurocognitive disorders persist in the era of potent antiretroviral therapy: CHARTER Study. Neurology. 2010; 75:2087–2096. [PubMed: 21135382]

Lancaster JL, Woldorff MG, Parsons LM, Liotti M, Freitas C, Rainey L, Kochunov PV, Nickerson D, Mikiten PA, Fox PT. Automated Talairach Atlas labels for functional brain mapping. Hum Brain Mapp. 2000; 10:120–131. [PubMed: 10912591]

Le Bihan DMJ, Poupon C, Clark CA, Pappata S, Molko N, Chabriat H. Diffusion tensor imaging: concepts and applications. J Magn Reson Imag. 2001; 13:534–546.

Letendre S, Marquie-Beck J, Capparelli E, Best B, Clifford D, Collier AC, Gelman BB, McArthur JC, McCutchan JA, Morgello S, Simpson D, Grant I, Ellis RJ. Validation of the CNS Penetration-Effectiveness rank for quantifying antiretroviral penetration into the central nervous system. Arch Neurol. 2008; 65:65–70. [PubMed: 18195140]

MacDonald CL, Dikranian K, Bayly P, Holtzman D, Brody D. Detects Experimental Traumatic Axonal Injury and Indicates Approximate Time of Injury. J Neurosci. 2007; 27:11869–11876. [PubMed: 17978027]

Mandonnet E, Nouet A, Gatignol P, Cappelle L, Duffau H. Does the left inferior longitudinal fasciculus play a role in language? A brain stimulation study. Brain. 2007; 130:623–629. [PubMed: 17264096]

Masliah E, DeTeresa RM, Mallory ME, Hansen LA. Changes in pathological findings at autopsy in AIDS cases for the last 15 years. AIDS. 2000; 14:69–74. [PubMed: 10714569]

Metwalli NS, Benatar M, Nair G, Usher S, Hu XP, Carew JD. Utility of axial and radial diffusivity from diffusion tensor MRI as markers of neurodegeneration in amyotrophic lateral sclerosis. Brain Res. 2010; 1348:156–164. [PubMed: 20513367]

McArthur JC, McDermott MP, McClernon D, St Hillaire C, Conant K, Marder K, Schifitto G, Selnes OA, Sacktor N, Stern Y, Albert SM, Kleburtz K, deMarcalda JA, Cohen RA, Epstein LG. Attenuated central nervous system infection in advanced HIV/AIDS with combination antiretroviral therapy. [erratum appears in Arch Neurol (2005) 62:1110]. Arch Neurol. 2004; 61:1687–1696. [PubMed: 15534180]

Mori, S.; Wakana, S.; Nagae-Poetscher, L.; van Zijl, PCM. MRI Atlas of Human White Matter. Elsevier; Amsterdam, the Netherlands: 2005.

Navia BA, Cho E-S, Petito CK, Price RW. The AIDS dementia complex: II. Neuropathology. Ann Neurol. 1986; 19:525–535. [PubMed: 3014994]

Parsons TD, Braaten AJ, Hall CD, Robertson KR. Better quality of life with neuropsychological improvement on HAART. Health Qual Life Outcomes. 2006; 24:4–11.

Pfefferbaum A, Rosenbloom MJ, Rohlfing T, Kemper CA, Deresinski S, Sullivan EV. Frontostriatal fiber bundle compromise in HIV infection without dementia. AIDS. 2009; 23:1977–1985. [PubMed: 19730350]

Pomara N, Crandall DT, Choi SJ, Johnson G, Lim KO. White matter abnormalities in HIV-1 infection: A diffusion tensor imaging study. Psychiatry Res. 2001; 106:15–24. [PubMed: 11231096]

Ragin AB, Wu Y, Storey P, Cohen BA, Edelman RR, Epstein LG. Diffusion tensor imaging of subcortical brain injury in patients infected with human immunodeficiency virus. J Neurovirol. 2005; 11:292–298. [PubMed: 16036809]

Rosas HD, Lee SY, Bender AC, Zaleta AK, Vangel M, Yu P, Fischi B, Pappu V, Onorato C, Cha JH, Salat DH, Hersch SM. Altered white matter microstructure in the corpus callosum in Huntington's disease: implications for cortical "disconnection". Neuroimage. 2010; 49:2995–3004. [PubMed: 19850138]

Smith SM, Jenkinson M, Woolrich MW, Beckmann CF, Behrens TEJ, Johansen-Berg H, Bannister PR, De Luca M, Drobnjak I, Flitney DE, Niazy RK, Saunders J, Vickers J, Zhang Y, De Stefano N, Brady JM, Matthews PM. Advances in functional and structural MR image analysis and implementation as FSL. Neuroimage. 2004; 23(S1):208–219.

Smith SM, Jenkinson M, Johansen-Berg H, Rueckert D, Nichols TE, Mackay CE, Watkins KE, Ciccarelli O, Cader MZ, Matthews PM, Behrens TE. Tract-based spatial statistics: Voxelwise analysis of multi-subject diffusion data. Neuroimage. 2006; 31:1487–1505. [PubMed: 16624579]

Smith SM, Nichols TE. Threshold-free cluster enhancement: addressing problems of smoothing, threshold dependence and localisation in cluster inference. Neuroimage. 2009; 44:83–98. [PubMed: 18501637]

Song SK, Sun SW, Ramsbottom MJ, Chang C, Russell J, Cross AH. Demyelination revealed through MRI as increased radial (but unchanged axial) diffusion of water. Neuroimage. 2002; 17:1429–1436. [PubMed: 12414282]

Sun SW, Liang HF, Le TQ, Armstrong RC, Cross AH, Song SK. Differential sensitivity of in vivo and ex vivo diffusion tensor imaging to evolving optic nerve injury in mice with retinal ischemia. Neuroimage. 2006; 32:1195–1204. [PubMed: 16797189]

Tate DF, Conley J, Paul RH, Coop K, Zhang S, Zhou WJ, Laidlaw DH, Taylor LE, Flanigan T, Navia B, Cohen RA, Tashima K. Quantitative diffusion tensor imaging tractography metrics are associated with cognitive performance among HIV-Infected patients. Brain Imaging Behav. 2010; 4:68–79. [PubMed: 20503115]

Tate DF, Sampat M, Harezlak J, Flecas M, Hogan J, Dewey J, McCaffrey D, Branson D, Russell T, Conley J, Taylor M, Schifitto G, Zhong J, Daar ES, Alger J, Brown M, Singer E, Campbell T, McMahon D, Tso Y, Matesan J, Letendre S, Paulose S, Guagh M, Tripoli C, Yiannoutsos C, Bigler D, Cohen RA, Guttman CR, Navia B, HIV Neuroimaging Consortium. Regional areas and widths of the midsagittal corpus callosum among HIV-infected patients on stable antiretroviral therapies. J Neurovirol. 2011; 17:368–379. [PubMed: 21556960]

Thompson PM, Dutton RA, Hayashi KM, Lu A, Lee SE, Lee JY, Lopez OL, Alzenstein HJ, Toga AW, Becker JT. 3D mapping of ventricular and corpus callosum abnormalities in HIV/AIDS. Neuroimage. 2006; 31:12–23. [PubMed: 16427319]

Thurnher MM, Castillo M, Stadler A, Rieger A, Schmid B, Sundgren PA. Diffusion-tensor MR imaging of the brain in human immunodeficiency virus–positive patients. AJNR Am J Neuroradiol. 2005; 26:2275–2281. [PubMed: 16219833]

Tyor WR, Glass JD, Griffin JW, Becker PS, McArthur JC, Bezman L, Griffin DE. Cytokine expression in the brain during the Acquired Immunodeficiency Syndrome. Ann Neurol. 1992; 31:349–360. [PubMed: 1586135]

Wesselingh SL, Power C, Glass JD, Tyor WR, McArthur Farber JM, Griffin JW, Griffin DE. Intracerebral cytokine messenger RNA expression in Acquired Immunodeficiency Syndrome dementia. Ann Neurol. 1993; 33:576–582. [PubMed: 8498837]

Wohlschlaeger J, Wenger E, Mehraein P, Weis S. White matter changes in HIV-1 infected brains: A combined gross anatomical and ultrastructural morphometric investigation of the corpus callosum. Clin Neurol Neurosurg. 2009; 111:422–429. [PubMed: 19185416]

Woods SP, Moore DJ, Weber E, Grant I. Cognitive neuropsychology of HIV associated neurocognitive disorders. Neuropsychol Rev. 2009; 19:152–68. [PubMed: 19462243]

Wu Y, Storey P, Cohen BA, Epstein LG, Edelman RR, Ragin AB. Diffusion Alterations in Corpus Callosum of Patients with HIV. AJNR Am J Neuroradiol. 2006; 27:656–60. [PubMed: 16552012]

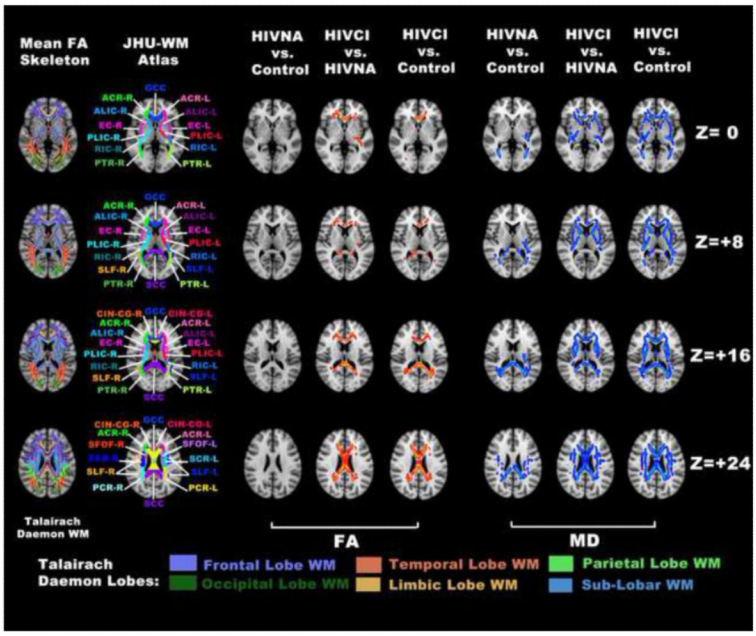

Fig. 1.

Voxelwise group comparisons using TBSS analysis revealed WM structures with significantly decreased FA (red clusters in 3rd to 5th column) and increased MD (blue clusters in 6th to 8th column) between controls and HIV infected subjects. The ICBM-DTI-81 White Matter Atlas from the Johns Hopkins University (JHU-WM Atlas) is superimposed on the MNI152 template for reference of white matter structures (2nd column). Each WM structures defined in the Atlas were labeled and the abbreviations used are the same as those defined in Table 2. The Talairach Lobe Template from Talairach Daemon (Lancaster et al. 2000) was also displayed to identify spatial distribution of the DTI abnormality within the white matter structure (1st column). Significant voxels within the skeleton are expended using the tbss_fill function of FSL package for better illustration. The same visualization approach is also applied in Fig. 2 and Fig. 3

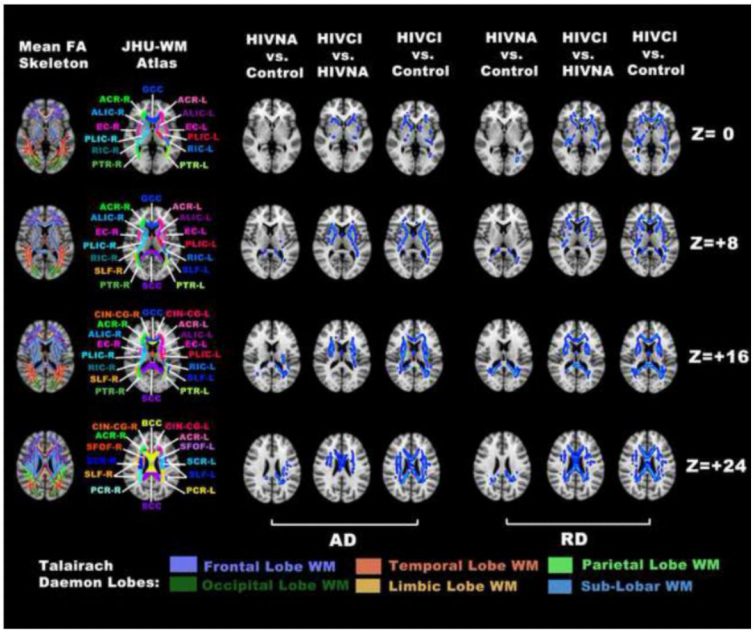

Fig. 2.

Voxelwise group comparisons using TBSS analysis as in Fig. 1 but restricted to significantly increased AD (blue clusters in 3rd to 5th column) and increased RD (blue clusters in 6th to 8th column)

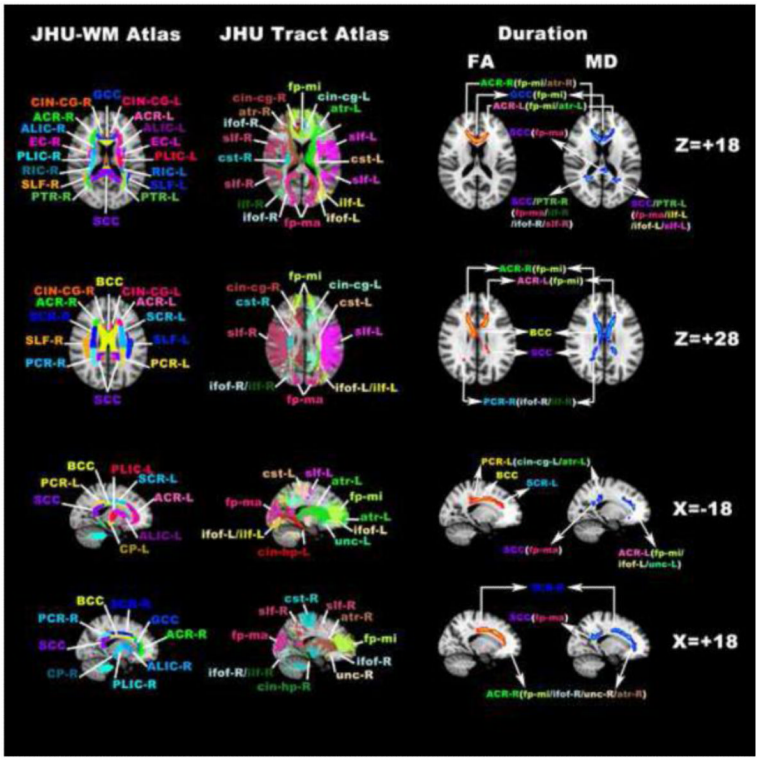

Fig. 3.

Voxelwise correlation analysis using TBSS analysis revealed WM structures/pathways in which FA/MD significantly correlated with the duration of HIV infection. Shown are 1) WM structures/tracts with significant correlations between decreased FA and the duration of infection (red clusters in 3rd column), and 2) WM structures/tracts with significant correlations between increased MD and the duration of infection (blue clusters in 4th column). The ICBM-DTI-81 White Matter Atlas (JHU-WM Atlas in 1st column) and the White Matter Tractography Atlas (JHU-Tract Atlas in 2nd column) from the John Hopkins University are superimposed on the MNI152 template for reference of WM structures as well as related WM fiber pathways. Each WM structures/pathways defined in the Atlas were labeled and the abbreviations used are the same as those defined in Tables 2 and 5

Table 1

Demographic characteristics

	Mean (± SD) or Frequency Count		
	Control (n=13)	**HIVNA (n=42)**	**HIVCI (n=8)**
Age	50.5(9.2)	47.6(7.7)	50.5(6.7)
Gender (M/F)	3/10	28/14	4/4
Race (Ethnicity White/Nonwhite)	12/1	23/19	4/4
Years of HIV Infection	N/A	10.7 (5.8)	15.1 (5.2)
Nadir CD4+	N/A	66.8 (42.7)	33.5 (39.5)
Current CD4+	N/A	386.3 (198.9)	230.4 (176.1)
Current CD4+<200mm^3	NA	5	4
Detectable plasma HIV RNA	N/A	9	3
Underwent cART treatment at the time of study	N/A	34	7

Table 2

White matter regions with significant DTI changes from TBSS analysis

WM Structures (JHU WM Atlas)	HIVNA vs. Control Skeleton_Abnorm%				HIVCI vs. HIVNA Skeleton_Abnorm%				HIVCI vs. Control Skeleton_Abnorm%			
	FA	MD	AD	RD	FA	MD	AD	RD	FA	MD	AD	RD
BCC	0	4.9	1.6	1.1	75.7	55.9	22.3	67.2	68.1	60.6	31.7	70.6
SCC	0	67.4	31.6	42.8	51.6	44.51	0	50.5	59.9	77.4	44.1	79.2
RIC-L	0	47.1	8.2	0	20.7	27.4	23.4	30.1	0	61.0	53.4	36.7
SCR-R	0	15.3	0	2.5	20.1	64.9	40.7	56.7	19.9	68.8	59.5	57.4
SCR-L	0	27.9	14.9	2.6	24.6	59.9	43.4	53.6	26.1	75.4	60.8	62.0
PCR-R	0	69.6	10.9	47.3	45.8	69.1	0	68.4	63.0	96.3	77.5	88.8
PCR-L	0	74.8	50.4	61.8	36.7	65.3	5.1	71.1	55.6	90.7	72.2	90.7
PTR-R	0	42.2	3.0	10.9	1.7	1.7	0	0.3	11.2	40.9	6.7	35.4
PTR-L	0	51.6	8.8	40.7	2.6	8.7	5.3	6.9	15.0	60.5	35.2	57.8
ILF/IFOF-R	0	4.2	0	0	0	12.7	3.1	14.4	0	32.4	0	12.5
ILF/IFOF-L	0	25.3	0	7.8	26.9	36.1	0.4	33.1	0	62.8	16.6	57.5
SLF-R	0	43.2	0.7	8.2	0	15.9	8.6	13.6	5.5	53.4	48.2	38.6
SLF-L	0	54.3	39.9	15.7	0.2	38.1	0.1	18.8	1.5	72.4	63.1	57.2
GCC	0	0	0	0	34.7	36.3	3.4	40.1	40.8	58.0	21.4	66.7
ALIC-R	0	0	0	0	0	61.3	48.2	42.6	0	57.7	52.4	40.2
ALIC-L	0	0	0	0	0	61.7	39.8	52.0	0	60.3	45.8	49.0
PLIC-R	0	0	0	0	0	37.4	23.1	17.1	0	48.0	45.0	27.9
PLIC-L	0	0	0	0	0.8	26.3	24.7	8.8	0	30.7	30.5	7.5
RIC-R	0	0	0	0	0	51.3	4.1	51.4	0	59.5	37.3	53.2
ACR-R	0	0	0	0	51.0	68.0	26.8	73.4	39.9	82.3	52.2	78.7
ACR-L	0	0	0	0	31.4	48.3	25.1	47.9	31.6	75.2	40.0	73.0
CIN-CG-R	0	0	0	0	21.3	19.1	6.9	20.1	17.9	27.3	0	30.8
CIN -CG-L	0	0	0	0	34.2	35.0	5.8	42.9	27.1	41.0	17.9	48.0
CIN-HP-R	0	0	0	0	0	0	0	0	0	12.8	0	8.1
CIN-HP-L	0	0	0	0	0	4.4	15.3	3.2	0	15.3	0	14.5
SFOF-R	0	0	0	0	0	65.8	50.0	61.8	0	53.9	43.4	40.8
SFOF-L	0	0	0	0	0	60.7	22.4	60.7	0	65.4	54.2	61.7

WM Structures (JHU WM Atlas)	HIVNA vs. Control Skeleton_Abnorm%				HIVCI vs. HIVNA Skeleton_Abnorm%				HIVCI vs. Control Skeleton_Abnorm%			
	FA	MD	AD	RD	FA	MD	AD	RD	FA	MD	AD	RD
UNC-L	0	0	0	0	0	80.0	43.6	70.9	0	52.7	9.1	70.9
EC-R	0	0	0	0	0	41.0	33.8	26.1	0	47.9	29.9	40.0
EC-L	0	0	0	0	9.2	69.7	49.9	57.4	0	77.1	42.9	70.9

Abbreviations (the same abbreviations are used for all tables and figures in the following):

L: left hemisphere; **R**: right hemisphere.

BCC: body of the corpus callosum; **GCC**: genu of the corpus callosum; **SCC**: splenium of the corpus callosum; **ALIC**: anterior limb of the internal capsule; **PLIC**: posterior limb of the internal capsule; **RIC**: retrolenticular part of the internal capsule; **EC**: external capsule; **ACR**: anterior corona radiata; **SCR**: superior corona radiata; **PCR**: posterior corona radiata; **CIN-CG**: cingulum at the Cingulate Gyrus; **CIN-HP**: cingulum at the hippocampus; **PTR**: posterior thalamic radiation; **ILF**: inferior longitudinal fasciculus; **IFOF**: inferior fronto-occipital fasciculus; **SLF**: superior longitudinal fasciculus; **SFOF**: superior fronto-occipital fasciculus. **UNC**: uncinate fasciculus.

Table 3

White matter structures with highest sensitivity and specificity where tensor-derived parameters differ between controls and HIVNA patients using logistic regression

WM Structures (JHU WM-Atlas)	DTI Parameters	AUC	Odds Ratio	Sensitivity	Specificity	Accuracy
SCC	**MD** ***	0.86	6.80	0.71	0.92	0.76
	RD ***	0.89	10.9	0.76	0.92	0.80
PTR-R	**MD** **	0.89	13.2	0.81	0.85	0.82
	RD ***	0.86	6.84	0.74	0.92	0.78
PTR-L	**MD** **	0.85	6.87	0.88	0.77	0.85
	RD **	0.86	6.07	0.90	0.77	0.87
SLF-L	**MD** **	0.87	11.10	0.90	0.85	0.99
	RD **	0.82	4.60	0.76	0.85	0.78

* Note: indicates $p<0.05$,

** indicates $p<0.005$,

*** indicates $p<0.001$ from the Wald test,

Table 4

White matter structures with highest sensitivity and specificity where tensor-derived parameters differ between HIVNA and HIVCI patients using logistic regression

WM Structures (JHU WM-Atlas)	DTI Parameters	AUC	Odds Ratio	Sensitivity	Specificity	Accuracy
BCC	**FA** **	0.86	0.15	0.88	0.81	0.82
	MD **	0.87	7.29	0.63	0.95	0.90
	RD **	0.85	5.60	0.75	0.86	0.84
CIN-CG-R	**MD** **	0.85	4.33	0.88	0.81	0.82
	RD **	0.82	4.28	0.88	0.81	0.82
CIN-CG-L	**MD** **	0.85	6.74	0.88	0.79	0.80
	RD *	0.83	4.42	0.88	0.91	0.90
ALIC-R	**MD** ***	0.90	7.14	0.75	0.95	0.92
	RD **	0.86	6.02	0.99	0.67	0.72
ALIC-L	**MD** **	0.97	21.67	1.00	0.93	0.94
	RD **	0.93	9.55	1.00	0.76	0.80
PLIC-R	**MD** **	0.94	9.70	1.00	0.81	0.84
	RD **	0.86	6.95	0.75	0.95	0.92
PLIC-L	**MD** **	0.90	7.03	0.88	0.86	0.86
	RD **	0.82	5.00	0.75	0.93	0.90
EC-R	**MD** **	0.88	4.89	1.00	0.71	0.76
	RD **	0.86	4.71	1.00	0.57	0.64
EC-L	**MD** **	0.91	5.52	1.00	0.76	0.80
	RD **	0.86	5.22	0.88	0.76	0.78

*Note: indicates $p<0.05$,

**indicates $p<0.005$,

***indicates $p<0.001$ from the Wald test,

Table 5

White matter structures/fiber pathways with significant correlations between FA/MD and duration of HIV infection

WM Structures (JHU WM Atlas)	FA (%)[a,b]	Associated WM Tracts[b] (JHU Tract Atlas)	MD (%)[a]	Associated WM Tracts[b] (JHU Tract Atlas)
GCC	32.4	*fp-mi, cin-cg-L, cin-cg-R*	45.5	*fp-mi, cin-cg-L, cin-cg-R*
BCC	27.3	*fp-mi, cin-cg-L, slf-R, slf-L, slf-tp-R, atr-L*	37.6	*fp-mi, cin-cg-L, atr-R, atr-L, slf-R, cin-cg-R, slf-L, slf-tp-R*
SCC	0.8	*cin-cg-L*	18.3	*fp-ma, cin-cg-L, cin-hp-R, cin-cg-R, cin-hp-L*
ACR-R	13.5	*fp-mi, cin-cg-R, slf-R, atr-R*	14.5	*fp-mi, cin-cg-R, slf-R, unc-R, atr-R, ifof-R*
ACR-L	14.2	*cin-cg-L, fp-mi*	20.4	*fp-mi, ifof-L, atr-L, cin-cg-L, unc-L*
SCR-R	10.5	*cst-R, atr-R, slf-R*	8.5	*atr-R, cst-R*
SCR-L	10.1	*cst-L, ,slf-L, cing-cg-L*	7.3	*slf-L*
PCR-R	1.8	*Ifof-R, ilf-R*	8.9	*Ifof-R, ilf-R, cin-cg-R, cin-hp-R, slf-R, fp-ma*
PCR-L	11.5	*cst-L, cin-cg-L, slf-L*	7.2	*cin-cg-L, ifof-L, slf-L*
EC-L	NA		4.0	*unc-L, ifof-L*
PTR-R	NA		2.4	*Ifof-R*
PTR-L	NA		1.9	*Ifof-L, ilf-L*

[a] For each WM structures in the table, the extent of significant correlation was quantified by the percentage value between the number of skeleton voxels with significant correlation within each structure and the total number of skeleton voxels of each structure, with a mathematical definition similar to Eq.1. For each WM structure, WM fiber pathways listed in the table follow the descending order according to the percentage of significant correlation voxels that belong to a specific WM tract.

[b] Abbreviations for fiber pathways (the same abbreviations are used for Table 5 as well as Fig. 3 and Fig. 4): Callosal fibers: **fp-mi** (forceps minor); **fp-ma** (forceps major); Association fibers: **cin-cg** (cingulum at the cingulate gyrus); **cin-hp** (cingulum at the hippocampus); **slf** (superior longitudinal fasciculus); **slf-tp** (superior longitudinal fasciculus at the temporal lobe); **ifof** (inferior fronto-occipital fasciculus); **ilf** (inferior longitudinal fasciculus); **unc** (uncinate fasciculus); Projection fibers: **cst** (corticospinal tract); **atr** (anterior thalamic radiation);

[c] NA indicates there are no significant correlation between FA/MD value and the duration of HIV infection at a specific WM structure.

Table 6

White matter structures with significant associations with cognitive deficit scores from multilinear regression analyses with model selection

WM Structures (JHU WM Atlas)	FA (beta value)		MD (beta value)	
	Speed of Info Processing	Verbal Fluency	Speed of Info Processing	Verbal Fluency
BCC	**– 0.026** *	−0.022	**0.048** *	0.060
SCC	−0.0096	−0.024	0.010	**0.041** *
ALIC-L	NA	NA	**0.021** ***	0.0083
ACR-L	**– 0.015** *	0.0053	0.014	0.0086
SCR-L	**– 0.016** *	−0.011	0.012	0.022
PCR-R	−0.0068	**– 0.0384** **	0.018	0.045
PCR-L	−0.0064	**– 0.045** ***	0.012	**0.058** *
ILF-IFOF-L	−0.0033	−0.010	0.0037	**0.053** *
EC-R	NA	NA	**0.015** *	0.012
EC-L	**– 0.015** *	−0.016	**0.016** *	0.0082
SLF-R	NA	NA	**0.027** *	0.031
SLF-L	−0.0057	−0.024	0.0074	**0.035** *
SFOF-R	NA	NA	**0.031** ***	0.011
SFOF-L	NA	NA	**0.019** *	0.0099

* Note: indicates $p<0.05$,

** indicates $p<0.005$,

*** indicates $p<0.001$, NA indicates that, at the corresponding ROI location, there was no significant FA/MD difference between HIVNA and HIVCI groups based on TBSS group comparisons.